62-3-4

REPORT NO. RR-TR-62-1
COPY 36

NEUTRONS PARTIAL CROSS SECTION STUDIES

10 APRIL 1962

aomc
U. S. ARMY ORDNANCE MISSILE COMMAND
REDSTONE ARSENAL, ALABAMA

AOMC FORM 1376, 1 MAR 62

10 April 1962 RR-TR-62-1

NEUTRONS PARTIAL CROSS SECTION STUDIES

By

D. R. Koehler and W. L. Alford

Department of the Army Project No. 599-04-002

Ordnance Management Structure Code No. 5610.11.703

RESEARCH LABORATORY

RESEARCH AND DEVELOPMENT DIRECTORATE

U. S. Army Ordnance Missile Command

ABSTRACT

The (n, 2n) excitation functions are given for Zn^{64}, Br^{79}, Ag^{107}, Sb^{121}, and Pr^{141}. Evidence is presented for a 7+ isomeric state in Y^{90} at 0.685 Mev. $Zr^{90}(n,p)Y^{90m}$ and $Nb^{93}(n,\alpha)Y^{90m}$ cross sections for 14.7-Mev neutrons are reported to be 12 ± 4 mb and 5 ± 2 mb, respectively.

TABLE OF CONTENTS

LIST OF ILLUSTRATIONS

NEUTRONS PARTIAL CROSS SECTION STUDIES

INTRODUCTION

The present state of nuclear reaction theory reflects the very primitive comprehension of the nucleus. The number of models employed in the reaction description is even more revealing evidence of this lack of understanding. To date the statistical model is one of the most common used; however, experimental results point to a restricted application and a direct interaction mechanism (Ref. 1) is frequently called upon to complement the description of the reaction process. Indeed, scientists generally agree that one of the basic tenets of the statistical compound nucleus structure is establishing highly chaotic nuclear conditions through absorbing an external agent (nucleon, γ-ray, etc.) with a subsequent loss of memory of the mode of excitation. Even this method appears questionable in some instances. Possible failure of the "thorough mixing" idea of compound nucleus theory has been discussed by Blatt and Weisskopf (Ref. 2). The action of the Pauli Exclusion Principle and the apparent existence of shell structure effects lead to fewer unoccupied states for energy transitions (leading to larger nucleon mean-free path) and weaker nucleon interaction within the nucleus (abandonment of quick energy sharing idea)(Ref. 3). Nonetheless the statistical model can be applied advantageously if only to demonstrate experimental deviations from theory.

Cross section studies of neutron induced particle emission processes constitute an area containing a paucity of experimental knowledge and this paper was prepared primarily to help fill this void. The (n, 2n) cross sections have been measured for Zn^{64}, Br^{79}, Ag^{107}, Sb^{121}, Pr^{141}, and Nb^{93} (Refs 4-7, 13). The need for a comprehensive knowledge of the decay scheme of the residual nuclei is a prime requisite for measurements which utilize the activation technique as employed in this work. This need has led to an independent determination of a new isomeric state of Y^{90} whose characteristics and production yields by (n, p) and (n, α) processes have been studied and will also be discussed (Refs. 7-13). Of secondary importance then, as a result of not having an adequate model with which to collate the experimental results, are the calculations of theoretical excitation functions. For the present work these computations were based on the aforementioned statistical model, a description which has been found by other workers to give a fair agreement with the experimental (n, 2n) cross section data.

THEORY

A more detailed description of the statistical model of nuclear reactions is necessary. Assuming the independence of the decay mode

upon the compound nucleus formation mode, the research scientists separate the cross section function as follows:

$$\sigma(a, b) = \sigma_c(a)G(b) \tag{1}$$

where $\sigma_c(a)$ is the cross section for formation of the compound nucleus by particle a and $G(b)$ is the probability that the compound nucleus will decay by emission of particle b. In the continuum or statistical theory (continuum in compound and residual nuclei) which represents an average over resonances, the first factor σ_c may be readily calculated. It is assumed that at the excitation energy of the compound nucleus, many levels of all types are involved. The corresponding wave functions will have random phases and averaging over these phases leads to noteworthy simplifications.

The probability of decay, $G(b)$, can also be calculated in this model which neglects phases between various excited levels of the compound nucleus if one assumes a continuously varying energy density, ω, of levels in the residual nucleus. $G(b)$ can be expressed as $\frac{\Gamma(b)}{\Sigma\Gamma_i}$ where Γ_i is the level width or decay probability into channel i. The channel concept is presented in more detail in Reference 2. Furthermore, by use of the reciprocity theorem (Ref. 2),

$$\Gamma(b) = k^2(b)\sigma(b) \tag{2}$$

where $k(b)$ is the wave number for particle b and is given by the expression

$$k(b) = \frac{M(b)}{\hbar}v(b). \tag{3}$$

Inasmuch as there are many decay channels that result in emission of particle b, if the incident particle energy is high enough to leave the residual nucleus in many excited states, $\Gamma(b)$ can be written as an integral

$$\Gamma(b) = \Gamma_b(\epsilon_{bY}) = \frac{2M_\beta}{\hbar^2}\int_0^{\epsilon_{bY}} \epsilon_\beta \sigma_c(\epsilon_\beta)\omega_Y(\epsilon_{bY} - \epsilon_\beta)\, d\epsilon_\beta = \sigma_c(\epsilon_\beta) \tag{4}.$$

is the cross section for formation of the compound nucleus by a collision with the energy ϵ_β between particles b and the excited nucleus Y^*, the latter having an excitation energy $\epsilon_{bY} - \epsilon_\beta$ and being the residual nucleus in the reaction $X(a, b)Y^*$. $\omega_Y(\epsilon_{bY} - \epsilon_\beta)$ is the level density function and furnishes the number of levels at the energy $\epsilon_{bY} - \epsilon_\beta$ of the residual nucleus Y^* in the energy interval $d\epsilon_\beta$. ω has also been calculated by statistical mechanical procedures (Ref. 3). The results are an exponential dependence on excitation

energy ω a exp $F(E)$. Thermodynamic analogies lead to a temperature concept and in particular a degenerate gas model yields the expression

$$\omega = C\exp 2(aE)^{1/2} \tag{5}$$

where C and a are constants depending on the mass number of the nucleus (Ref. 2). C is dependent on the odd, even character of the nucleus and for the calculation here the relation C odd odd = 2.4 C even odd = 12 C even even has been used (Ref. 14).

The temperature concept referred to manifests itself in the energy distribution of the particles emitted from the compound nucleus. The statistical procedures outlined result in a Maxwellian energy distribution where the temperature of the source is given by

$$\theta = \left(\frac{E}{a}\right)^{1/2}; \tag{6}$$

a is the constant in the level density function and E is the energy of excitation of the residual nucleus. Some experimental results indicate a lower "temperature"; that is, a lower energy maximum than the theory predicts. It appears that the fault lies in ω; there are fewer low-lying levels and more high levels than indicated by an exponential function (Ref. 15). Our cross section function now has the form

$$\sigma(a, b) = \sigma_c(a)\frac{\Gamma(b)}{\sum_i \Gamma_i} \tag{7}$$

where the Γ's are given above in equation (4).

An approximate cross section expression can be derived for the (n, 2n) process if certain reasonable assumptions are made. In considering the (n, 2n) reaction, the $\Gamma(b)$ function in equation (4) represents a probability for neutron emission; however, the integral includes only those cases in which the intermediate nucleus, after emission of the first neutron, is sufficiently excited to emit the second neutron. A common assumption is that the intermediate nucleus will emit the second neutron if the excitation energy is sufficient. Under this assumption then, the probability of the (n, 2n) process can be viewed as the difference between the total probability of neutron emission and the probability that the intermediate nucleus will <u>not</u> be excited enough to emit a second neutron.

Stated in mathematical form

$$\sigma(n, 2n) = \left[\frac{\int_0^{E_n} \epsilon_n \sigma_c(\epsilon_n)\, \omega_Y (E_n - \epsilon_n) d\epsilon_n}{\sum_i \Gamma_i} - \frac{\int_{\epsilon_{sec}}^{E_n} \epsilon_n \sigma_c (\epsilon_n) \omega_Y (E_n - \epsilon_n) d\epsilon_n}{\sum_i \Gamma_i} \right] \tag{8}$$

where E_n is the energy of the incident neutron and ϵ_{sec} is the maximum energy the first emitted neutron can have and still allow the emission of a second neutron. The above expression can be written as

$$\sigma(n, 2n) = \sigma_c(n) \left[\frac{\int_0^{\epsilon_{sec}} \epsilon_n \sigma_n(\epsilon_n) \omega_Y (E_n - \epsilon_n) d\epsilon_n}{\sum_i \Gamma_i} \right] \tag{9}$$

A further simplification results from neglecting processes other than neutron emission (Ref. 15). In this instance, the denominator becomes

$$\int_0^{E_n} \epsilon_n \sigma_c(\epsilon_n) \omega_Y (E_n - \epsilon_n) d\epsilon_n \tag{10}$$

For $E_n - E_{th} > \theta$, the above expression can be approximately written as (see Appendix)

$$\sigma(n, 2n) = \sigma_{in}(E_n) \left[1 - \left(1 + \frac{\epsilon_c}{\theta} \right) \exp\left(- \frac{\epsilon_c}{\theta} \right) \right] \tag{11}$$

Where ϵ_c is the excess energy over the threshold of the (n, 2n) reaction ($\epsilon_c = E_n - E_{th}(n, 2n)$) and θ is the nuclear temperature of the intermediate nucleus as defined earlier. This approximation expression was the one used to calculate the theoretical (n, 2n) excitation functions presented in the following text (with the exception of the calculations for zinc).

EXPERIMENTAL PROCEDURE

With the Research Laboratory 2-Mev Van de Graaff accelerator as a source of deuterons, neutrons in the energy range from 12.2 to 18.3 Mev were produced by utilizing the $T(d, n)He^4$ reaction. The target was 300 $\mu g/cm^2$ of tritium impregnated zirconium on a 0.25-mm platinum backing and was obtained from the Oak Ridge National Laboratory. Since He^4, the residual nucleus in this neutron producing reaction, has no excited states below 20 Mev, this reaction provides a source of monoenergetic neutrons. Variation of neutron energy was effected by the choice of angle for irradiation and by variation of the incident deuteron energy. Another nuclear reaction used for neutron production was the $Be^9(d, n)B^{10}$ reaction, which with deuterons of 2 Mev produced neutrons of energy less than 6.4 Mev. Although this source does not produce monoenergetic neutons, it does provide an intense flux ($\sim 10^9$ n's/μa sec) of neutrons. The water-cooled beryllium target used in these experiments was purchased from High Voltage Engineering Corp. An important consideration in using gas-occluded targets is cooling. For the tritium targets cooling was accomplished in one case by directing a jet of nitrogen on the platinum backing and for the second tritium target by circulating water over the back face of the platinum. The water layer behind the target was only $^1/_{64}$ inch and thus introduced negligible attenuation of the neutron flux. Beam currents were restricted to less than 4 microamperes for the gas-cooled tritium target and to less than 10 microamperes for the water-cooled tritium target as an additional safeguard against tritium loss; however, up to 30 microamperes of deuterons could be used with the beryllium target.

The water-cooled tritium target and sample irradiation apparatus are shown in Figure 1. This apparatus was designed to keep the mass in the vicinity of the target to a minimum to reduce neutron scattering and absorption. The samples were positioned in a horizontal plane passing through the beam axis and could be located about the target at any 10-degree interval from 0° to 160° and at distances of 2, 3, or 4 inches. When using 0.3-Mev deuterons on the tritium target, the spread in neutron energies for 0° to 90° is only 1.4 Mev (in 14.7 Mev). With this energy spread which is tolerable, a sample can be placed immediately adjacent to the target, thus subtending a large solid angle and increasing the neutron flux seen by the sample. The niobium and zirconium activations were done in this way.

Excitation function measurements were made by an activation technique wherein the residual radioactivity resulting from the (n, 2n) reaction was observed. The relative cross sections were determined by simultaneously irradiating four samples and subsequently measuring the induced beta activity in four shielded Geiger counters of window thickness

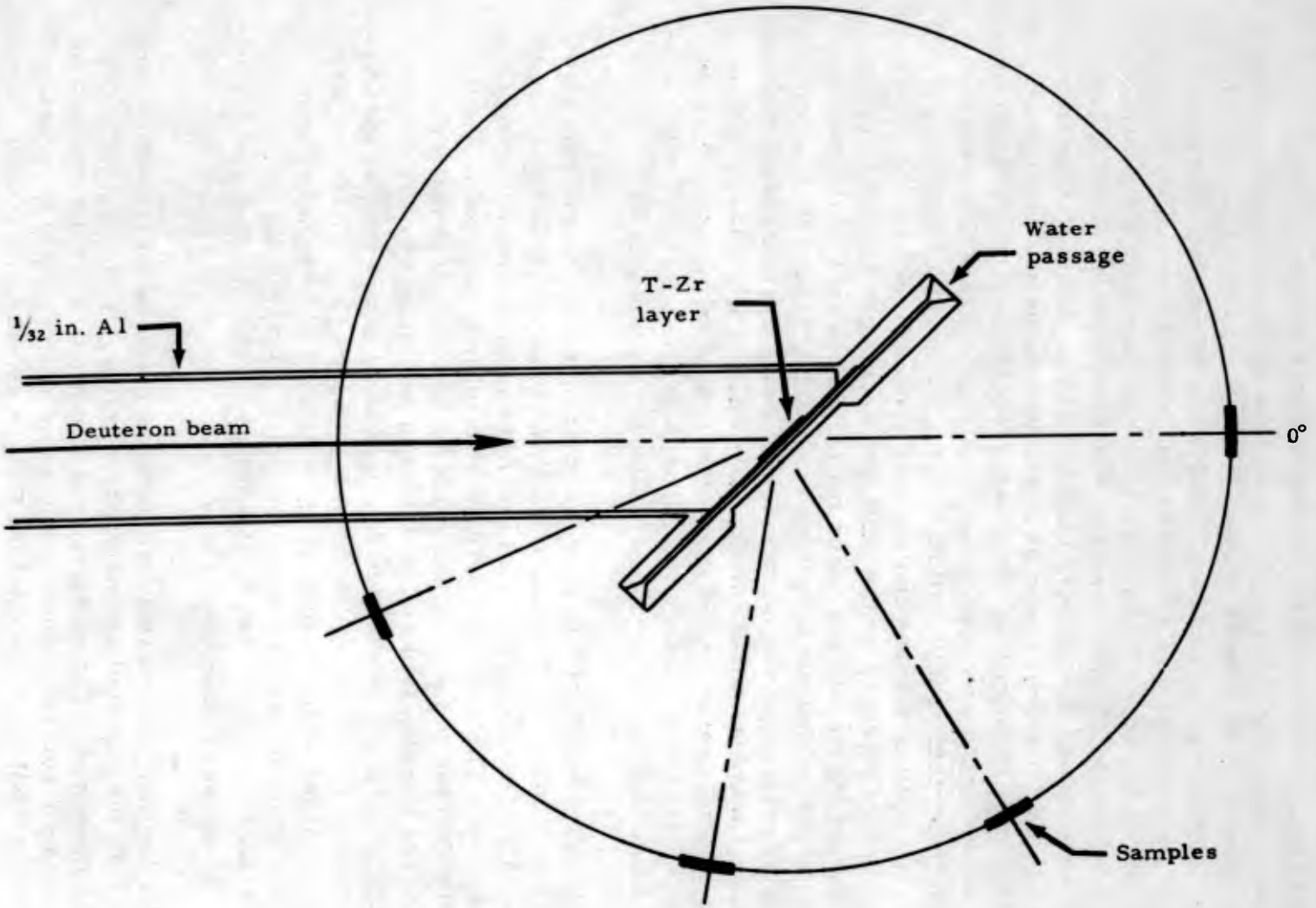

Figure 1. - Target and sample apparatus.

1.6 to 2.0 mg/cm^2. The counters fed an event recorder which produced a permanent record of sample activity as a function of time. The information was then plotted, the decay curves analyzed, and initial activities determined. The activities thus measured, after applying appropriate neutron flux correction factors, provided a measure of the cross sections. The differential cross section measurements of Bame and Perry (Ref. 16) were used in order to correct for variations in neutron yield with angle. To reduce the errors arising from small differences in samples (less than 1 per cent by weight) and in counter efficiencies (approximately 5 per cent by calibration standard), the following technique was used. For a given choice of four sample positions, and the corresponding neutron energies, four runs were made. Each sample was assigned to a particular counter and during the course of the experiment was counted only by this particular counter. Sample position, however, was permuted for each run. This procedure resulted in each sample being exposed to the four neutron energies and subsequently each counter counting an activity induced by each of the four neutron energies.

For the $Nb^{93}(n,\alpha)Y^{90m}$, the $Nb^{93}(n,2n)Nb^{92}$, and the $Zr^{90}(n,p)Y^{90m}$ cross section measurements, a gamma ray counting technique was used. For the $Nb^{93}(n,\alpha)Y^{90m}$ and the $Nb^{93}(n,2n)Nb^{92}$ mesaurements, the niobium sample was sandwiched between disks of copper foil and activated. A comparison was made of the yield of the Y^{90m} and Nb^{92} gamma rays and the annihilation gammas from Cu^{62}. The $Zr^{90}(n,p)Y^{90m}$ cross section was determined by comparing the total counts under the Y^{90m} gamma photopeaks and the 0.915-Mev photopeak from Zr^{89}. Gamma rays were detected by two NaI(Tl) crystals, $2\frac{1}{2}$ inches in diameter and 2 inches thick, coupled to DuMont 6363 photomultiplier tubes in conjunction with two single channel analyzers. Other instrumentation used in the gamma-ray measurements were a coincidence circuit of 0.1 μsec resolving time and a Radiation Counter Laboratory Inc. 256 channel analyzer.

Irradiation times were approximately two half lives of the pertinent residual activity except for the niobium and zirconium activations which were restricted to one hour. The samples were rectangular sheets of reagent grade zinc (99.99 per cent) and pure silver (99.9 per cent), rectangular pellets of Pr_2O_3 (99.8 per cent), rectangular pellets of reagent grade sodium bromide coated with Formvar to reduce the rate of moisture absorption, and reagent grade Sb_2O_3 encapsulated in circular plastic planchets. The samples of niobium metal powder (99.92 per cent pure) and zirconium hydride powder (99.8 per cent pure, reactor grade) as well as the separated isotope samples of Zr^{90} oxide (98.66 per cent enriched) and Zr^{92} oxide (93.22 per cent enriched) were likewise encapsulated in plastic planchets for irradiation. The thicknesses of the rectangular samples were approximately equal to the range of the associated beta particle.

Each sample consisted of two such rectangular pieces placed back to back when being irradiated and side by side when being counted. In this manner, a larger mass was exposed to the neutrons with no loss in detectable beta activity due to the added thickness of sample material.

Chemical separations (Ref. 17) were carried out following irradiation of the niobium and zirconium samples, however no chemistry was performed when the separated isotopes of zirconium were employed. The niobium samples were dissolved in concentrated nitric and hydrofluoric acids; yttrium and zirconium carriers were added with the yttrium precipitating as the fluoride. For beta counting under thin window Geiger counters and for gamma ray coincidence measurements, the yttrium precipitate was metathesized with 10 molar potassium hydroxide, washed, dissolved in hydrochloric acid, and evaporated to dryness. The irradiated zirconium samples were dissolved in dilute hydrofluoric acid after which the process was the same as for the niobium samples.

RESULTS AND DISCUSSION

Excitation functions have been measured for the following reactions: $Zn^{64}(n, 2n)Zn^{63}$, $Br^{79}(n, 2n)Br^{78}$, $Ag^{107}(n, 2n)Ag^{106}$, $Sb^{121}(n, 2n)Sb^{120m}$, and $Pr^{141}(n, 2n)Pr^{140}$. In addition to these excitation function measurements, the values of the following cross sections have been determined at 14.7-Mev neutron energy: $Nb^{93}(n, 2n)Nb^{92}$; $Nb^{93}(n, \alpha)Y^{90m}$; $Zr^{90}(n, p)^{90m}$. Prior to making these latter three measurements, the characteristics of the isomeric state of Y^{90} were carefully studied in order to provide the decay scheme information necessary to the cross section measurements.

Excitation Functions

The measured excitation functions are shown in Figures 2 through 6. In these figures, the neutron energy spread is shown as a horizontal bar. The main source of this spread was due to sample size (angular spread) since the thickness of the zirconium layer corresponded to only small energy decrements from 36 to 49 Kev for the incident deuterons. Estimates of standard deviations, which amount to approximately ± 9 per cent, are indicated by vertical lines except where noted otherwise. Sources of error considered in these estimates were: (1) uncertainty in geometry and sample size; (2) uncertainty in counting efficiencies; (3) contribution due to scattered and absorbed neutrons; (4) the statistical error in counting; and (5) the error in the angular distribution of neutrons from the $T(d, n)He^4$ reaction as measured by Bame and Perry (Ref. 16). The indicated standard deviations do not include the errors due to the conversion from relative to absolute cross section.

Figure 2 shows a composite of the experimental results obtained for the $Zn^{64}(n, 2n)Zn^{63}$ cross section. The energy interval from 12.2 to 18.1

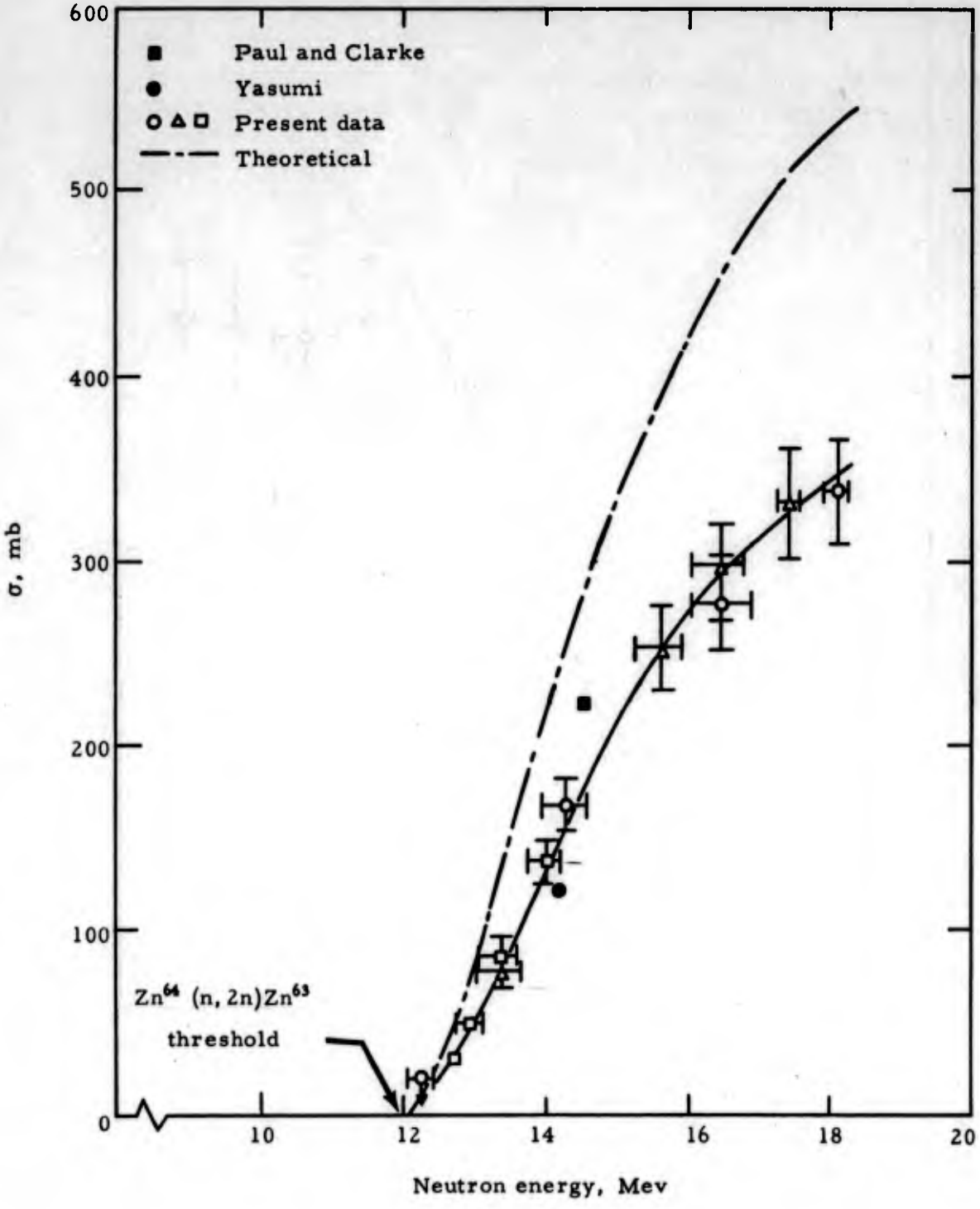

Figure 2. - The experimental Zn^{64} (n, 2n) Zn^{63} cross section as a function of incident neutron energy. The present data are indicated by the symbols O, Δ, and □; each symbol representing the averaged results for one particular choice of four neutron energies, and corresponding to deuteron energies of 2.0, 1.5 and 0.8 Mev, respectively. The point at 12.2 Mev represents an upper limit for the cross section value.

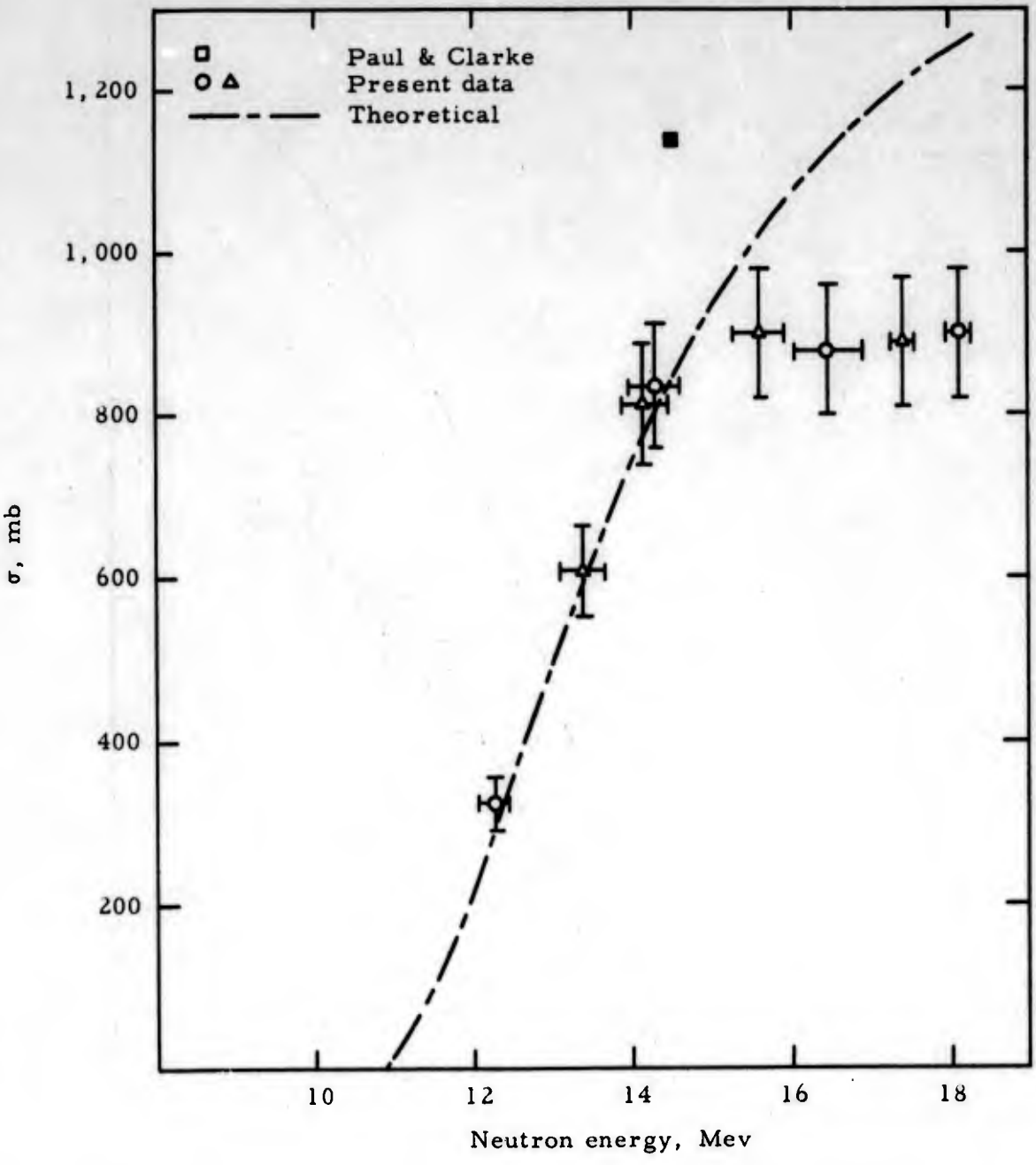

Figure 3. - Br^{79} (n, 2n) Br^{78} excitation function.

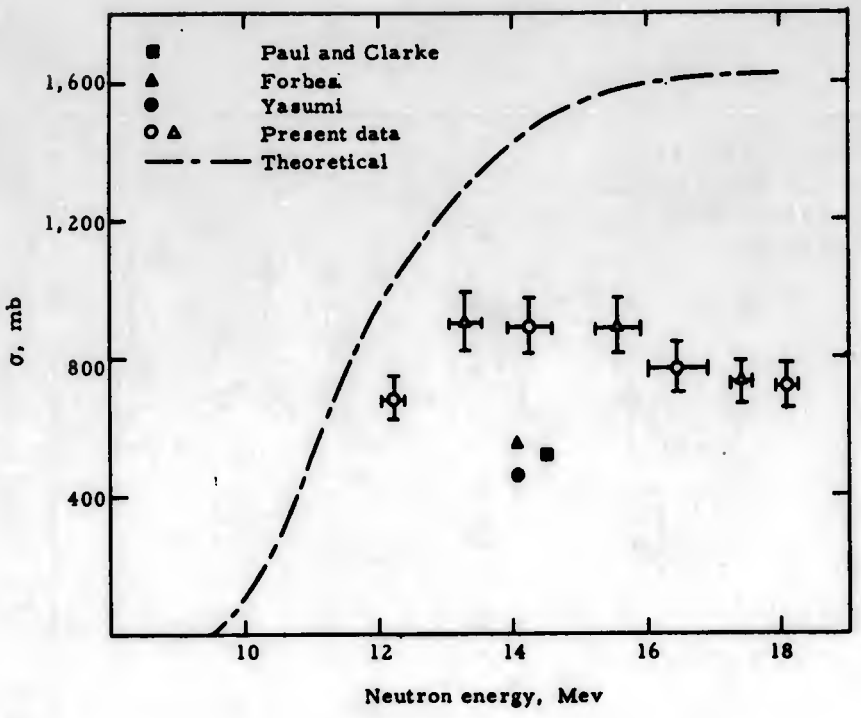

Figure 4. - Ag^{107} (n, 2n)Ag^{106} excitation function.

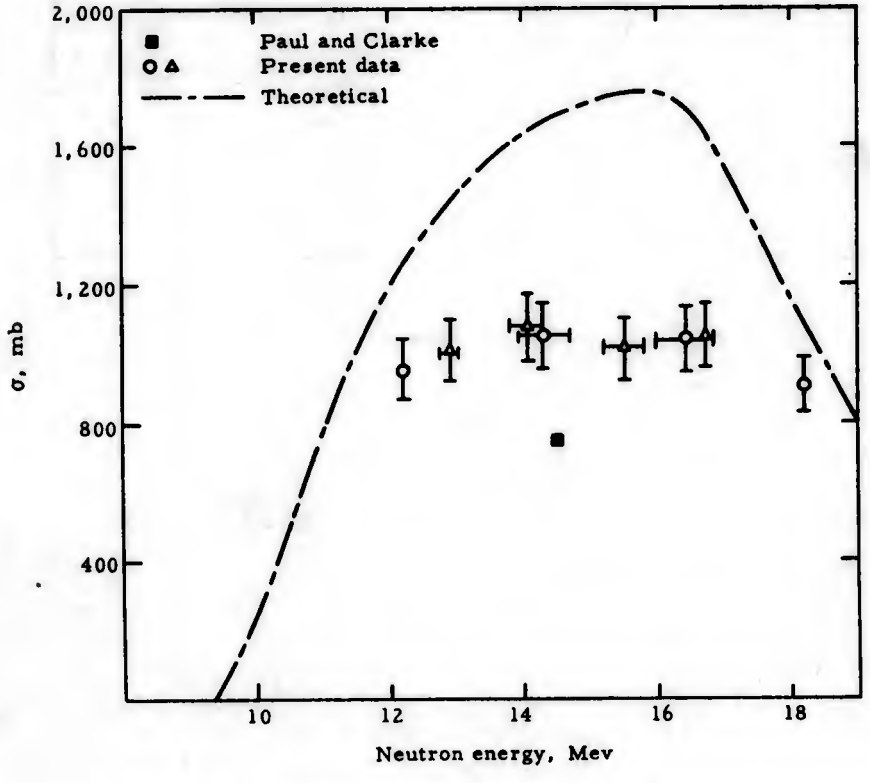

Figure 5. - Sb^{121} (n, 2n) Sb^{120} excitation function.

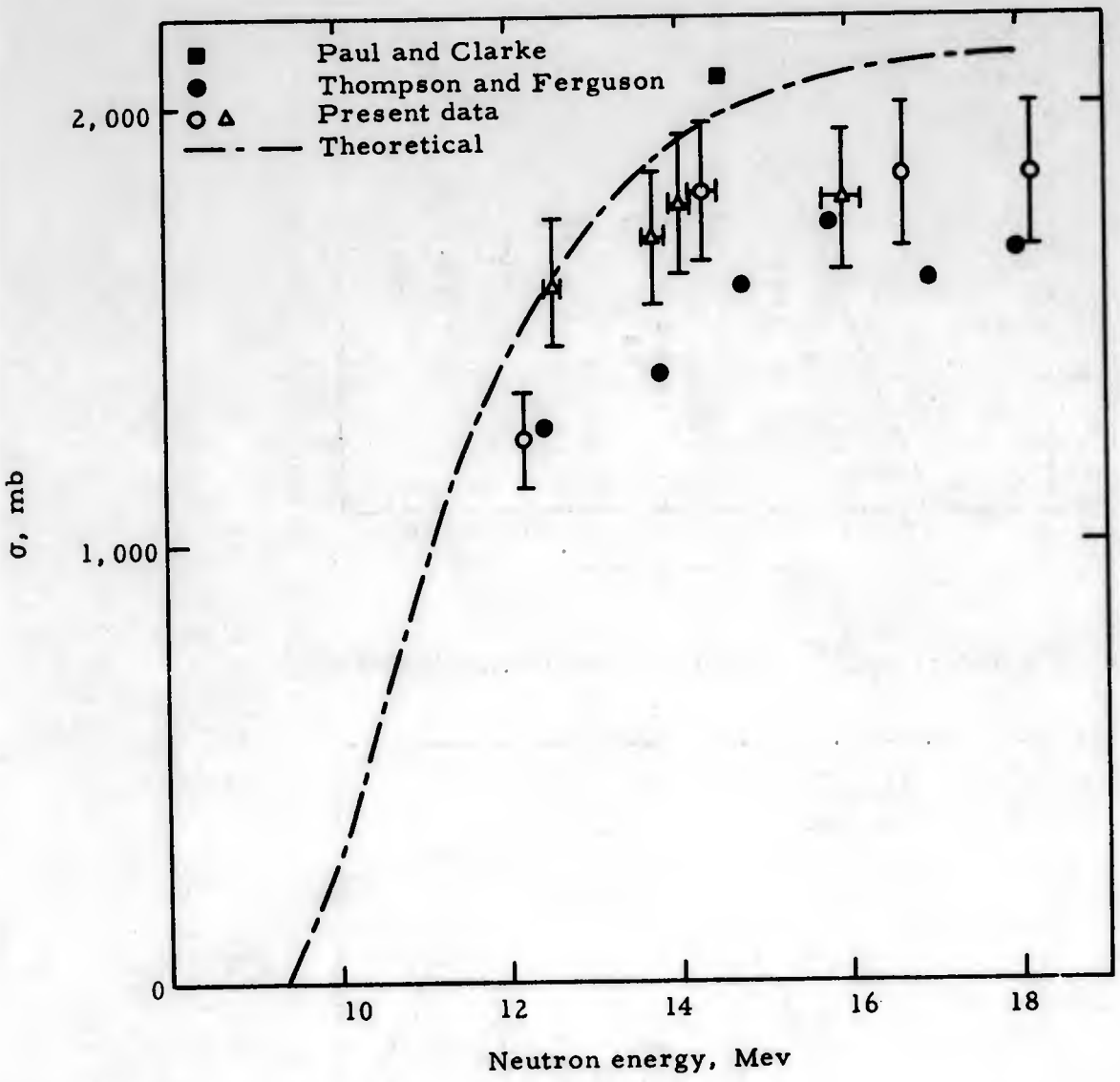

Figure 6. - Pr^{141} (n, 2n) Pr^{140} excitation function.

Mev was spanned by three sets of data, each set consisting of four neutron energies. These three sets corresponded to deuteron energies of 2.0, 1.5, and 0.8 Mev. Smooth curves were drawn through the cross section results of each set, and each curve was subsequently assigned an absolute scale by normalizing to Rayburn's value of 167 mb at 14.4 Mev (Ref. 18). The cross sections as measured at 14.1 Mev and 14.5 Mev by Yasumi (Ref. 19) and Paul and Clarke (Ref. 20), respectively, are also indicated. The theoretical excitation function was calculated according to equation (7) and is presented as the dashed curve. In the level density function $\omega(E) = C \exp 2(aE)^{1/2}$ the value of $a = 2.0$ (Ref. 15) was used and a value of 12 was employed for the ratio of C odd odd to C even even (Ref. 14). For these calculations the cross sections for compound nucleus formation were taken from Blatt and Weisskopf (Ref. 2) assuming $r_o = 1.5\,(10)^{-13}$ cm. Neutron and proton branching probabilities were calculated by numerical integration and other possible competing reactions were neglected. The computations leading to the theoretical curve include a nonnegligible contribution from the $Zn^{64}(n, p)Cu^{64}$ decay channel which results in a departure from the usual behavior of (n, 2n) cross sections where neutron emission is predominant when energetically possible. In general the qualitative results of these cross-section measurements agree well with those of Cohen and White (Ref. 21).

The theoretical excitation functions, presented with the experimental values, in Figures 3 through 6 were calculated with equation (11). The a values, as for the Zn calculations, were taken from Reference 15. Although no experimental results are available for (n, p) and (n, α) reactions on Br^{79}, the more exact expression, equation (7), which takes into account these competing reactions, yields an excitation function which differs negligibly from the results shown in Figure 3, which were calculated with the approximate expression (equation 11). The experimental and theoretical results are in good agreement from threshold to about 14.5 Mev. The absolute scale for the experimental curve was obtained by using the previously measured value of 835 mb at 14.4 Mev (Ref. 18). Also shown is Paul and Clarke's value at 14.5 Mev (Ref. 20).

The $Ag^{107}(n, 2n)Ag^{106}$ cross sections, normalized to Rayburn's value (Ref. 18) of 889 mb, are presented in Figure 4 along with the results reported by Forbes (Ref. 22) (560 mb ± 10 per cent), Yasumi (Ref. 19) (458 mb ± 11 per cent), and Paul and Clarke (Ref. 20) (519 mb ± 50 per cent). These experimental results should not be compared directly with the theoretical values since they represent an experimental cross section for the production of the 24-minute state of Ag^{106} only.

Figure 5 shows the cross-section results for the $Sb^{121}(n, 2n)Sb^{120}$ reaction. These results represent the cross section for the (n, 2n) reaction leading to the 17-minute component of the Sb^{120} isomeric pair. The value of 1056 mb (Ref. 18) was used to normalize the experimental relative excitation function. Paul and Clarke's result (Ref. 20) at 14.5 Mev is also indicated. The decrease observed above 17 Mev is probable evidence of the onset of the (n, 3n) reaction. This decrease is also apparent in the theoretical cross section curve which takes account of the (n, 3n) reaction with a threshold at 16.0 Mev (Ref. 23).

The $Pr^{141}(n, 2n)Pr^{140}$ experimental and theoretical cross section results are shown in Figure 6. Again the experimental values were normalized to Rayburn's value of 1591 mb (Ref. 18). Ferguson and Thompson's (Ref. 24) experimental excitation function is also presented for comparison in addition to Paul and Clarke's value at 14.5 Mev. (Ref. 20). The more rapid rise (as opposed to a smaller nucleus, e.g. Zn^{64}) and approach to the plateau of the excitation function can be understood in terms of the greater density of levels available to larger nuclei. In other words, for a given excitation energy, the larger (greater A) nucleus has more channels open to decay and consequently a larger fraction of the nonelastic neutron cross section will be observed for the (n, 2n) process.

Isomerism of Y^{90}

The recently reported activity induced by bombarding niobium with 14-Mev neutrons has been studied and has been shown to be due to an isomeric state of Y^{90} arising from the $Nb^{93}(n, \alpha)Y^{90m}$ reaction (Ref. 25). Two coincident gamma rays having energies of 0.485 and 0.200 Mev decaying with a 3.1 ± 0.1 hour half-life have been observed in agreement with previous measurements. The results obtained for 14.7 ± 0.7 Mev neutrons on niobium are shown in Figure 7. Prior to chemical separation the niobium gamma spectrum showed, in addition to the well known gamma ray at 0.930 Mev from Nb^{92}, two other gammas at 0.200 and 0.485 Mev (Ref. 26). The spectra shown in Figure 7 for the yttrium fluoride precipitate and for the supernatant solution indicate a satisfactory chemical separation. The decay of both the 0.485 and 0.200 Mev gammas was studied by following the output of single-channel analyzers set to pass pulses occurring within the two photoelectric peaks in two back-to-back NaI crystals. Measurements on both gammas covering a period of about 15 hours gave a value of 3.1 ± 0.1 hours for the half-life of each. The coincidence counting rate was also followed and the same half-life was obtained. Additional gamma spectra were recorded on the multichannel analyzer gated by

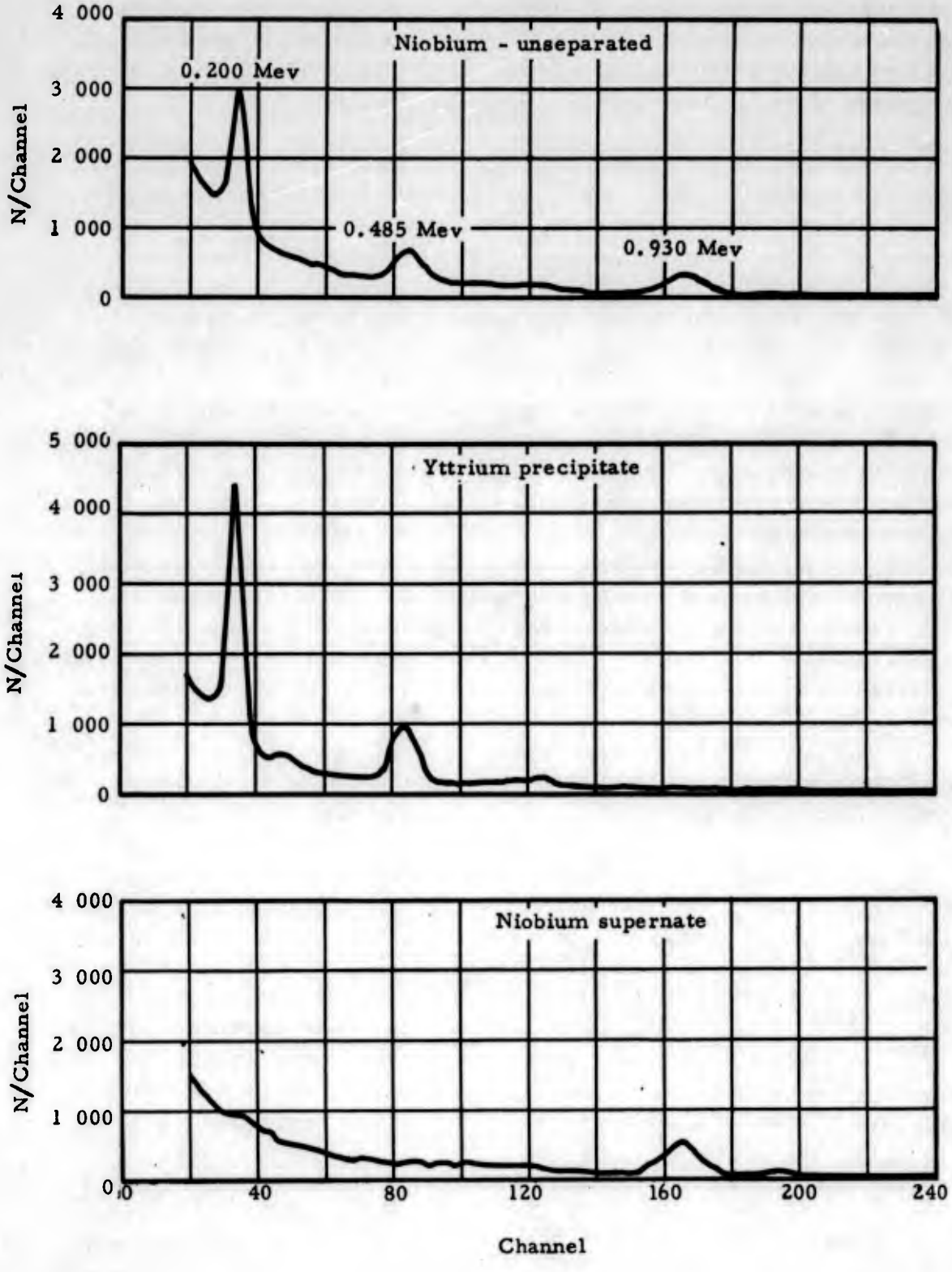

Figure 7. - Gamma ray spectra resulting from niobium activation with 14.7-Mev neutrons.

the output of the coincidence circuit. The gating pulse required coincidence between the output of the two NaI crystals and the output of a single channel analyzer. Spectra were recorded on the multichannel analyzer with the single channel set at 0.200 Mev and at 0.485 Mev. The spectra showed these gammas to be in coincidence.

The decay of the yttrium fraction was also followed by a thin window Geiger counter. The sample decayed with a half-life of approximately 65 hours, a value matching that of the beta decay of Y^{90}. Observation of a buildup of the 65-hour decay due to the possible 3.1-hour isomeric state was unsuccessful; however, the low yield of Y^{90m} and the delay due to chemical separations would make this difficult.

The results for 14.7 Mev neutrons on zirconium are shown in Figure 8. Here again the chemical separation points to an isotope of yttrium as the source of the 0.200- and 0.485-Mev gammas; this result is in agreement with the niobium data. Present in the spectrum from the supernatant solution of zirconium are prominent gamma rays at 0.388, 0.511 and 0.915 Mev. The 0.511- and 0.915-Mev gamma rays are attributed to the decay scheme of Zr^{89} resulting from an (n, 2n) reaction in Zr^{90}. The 0.388-Mev gamma ray is expected from the $Zr^{90}(n, \alpha)Sr^{87}$ reaction. The 0.551-Mev gamma which arises from the yttrium fraction, along with the 0.200- and 0.485-Mev gammas is attributed to Y^{91} formed by $Zr^{91}(n, p)$. The decay of the yttrium fraction was followed by the Geiger counter with a resulting decay curve which could be resolved into 65- and 3.5-hour components. These components could be accounted for by the beta decay of Y^{90} and Y^{92}.

Samples of niobium and zirconium were also bombarded by neutrons of energy less than 6 Mev produced by 1.7-Mev deuterons on a beryllium target; the neutron energy was below the $Nb^{93}(n, 2p)$, $Nb^{93}(n, He^3)$, Zr (n, d) and Zr(n, t) thresholds (Refs. 23 and 27). The fact that the activity was still observed in the niobium bombardment indicates either a $Nb^{93}(n, \alpha)Y^{90m}$ or a $Nb^{93}(n, n'\alpha)Y^{89m}$ reaction. The known properties of Y^{89m} essentially eliminate the latter reaction as a possibility. Furthermore, the fact that the activity is produced in the zirconium bombardment completely eliminates Y^{89m} as the responsible activity.

Since gammas similar to those presently considered have been previously attributed to levels in Zr^{92} from the decay of Y^{92}, separated isotopes of Zr^{90} and Zr^{92} were bombared by 14.7-Mev neutrons. Irradiation of Zr^{90} gives rise to the spectrum of Figure 9. Apparently present in this spectrum are the 0.388-Mev gamma ray from Sr^{87m}, 0.200- and 0.485-Mev gamma rays from Y^{90m} and those gammas from

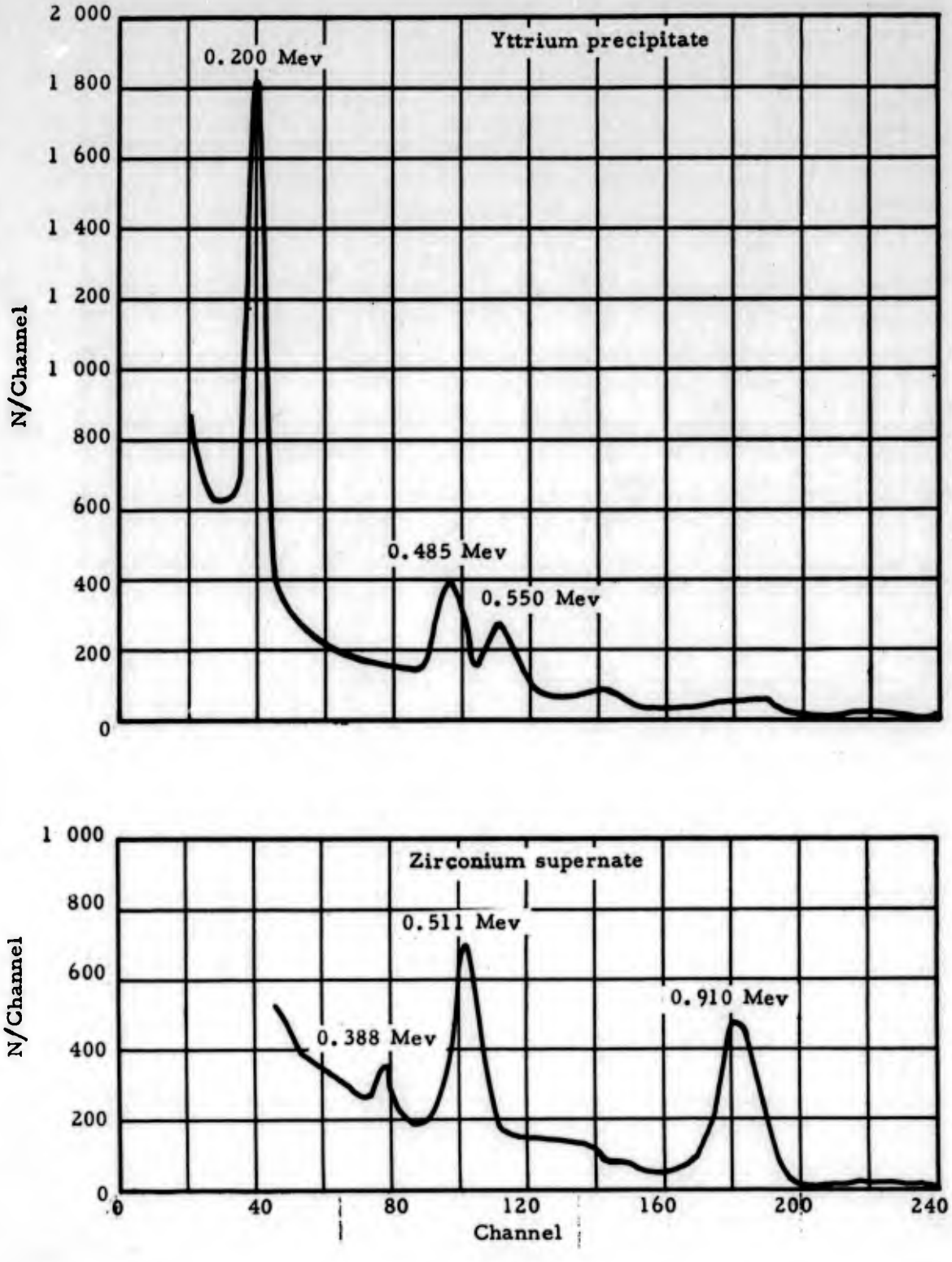

Figure 8. - Gamma ray spectra resulting from zirconium activation with 14.7-Mev neutrons.

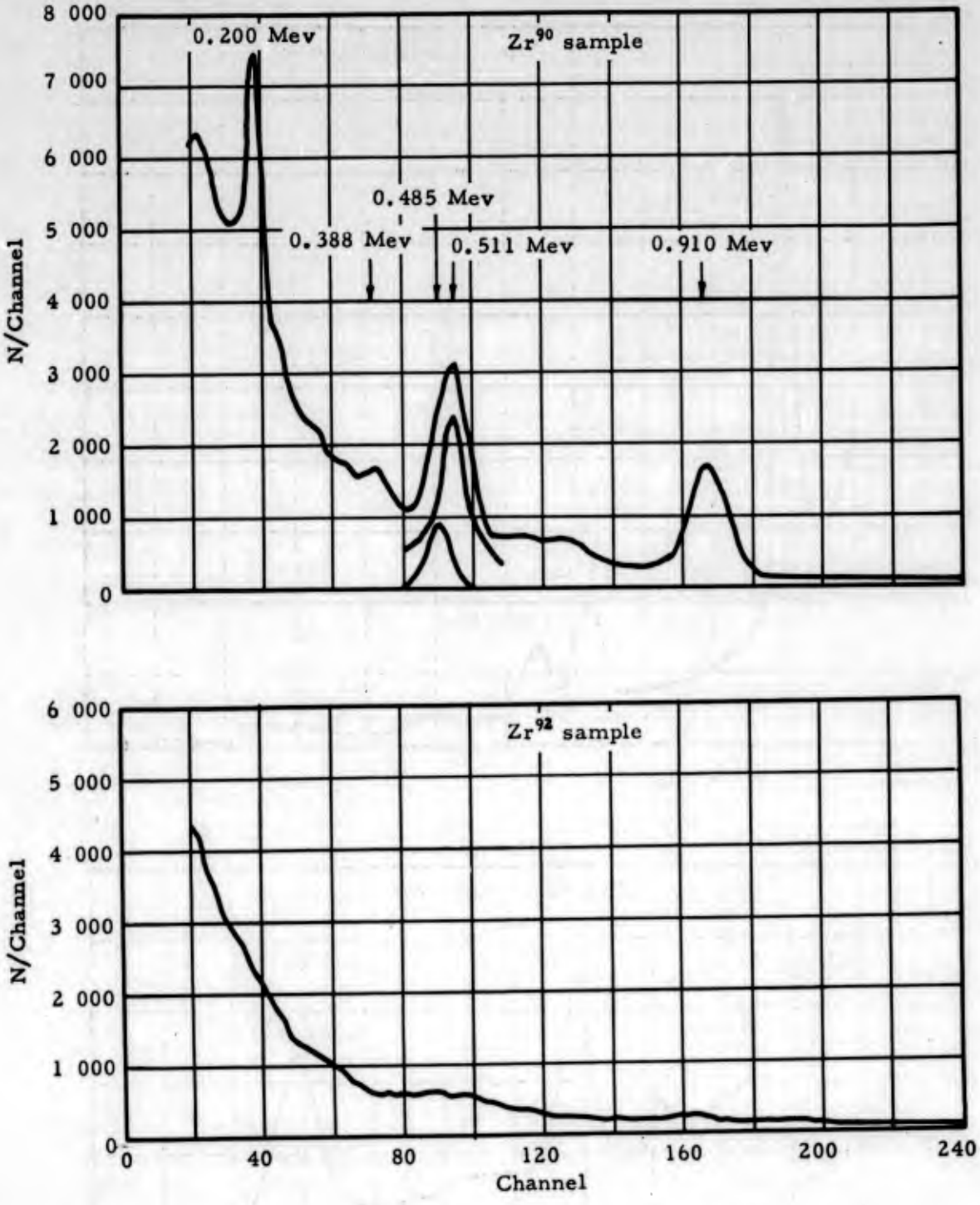

Figure 9. - Gamma ray spectra resulting from 14.7-Mev neutron activation of Zr^{90} and Zr^{92}. The structure of the peak near 0.500 Mev in the Zr^{90} spectrum was deduced by observing the 0.511-Mev peak of the 79-hour Zr^{89} after the 3.1-hour activity had decayed away.

the decay of Zr^{89}. The assumption that the peak near 0.5 Mev is due to a mixture of 0.485- and 0.511-Mev gammas appears reasonable from the width of the peak. This spectrum was taken after sufficient time had elapsed for the decay of the 4.4 minute Zr^{89m}. A subsequent Geiger count followed a rate of decay which could be attributed to a mixture of Y^{90} (65 hours) and Zr^{89} (79 hours). There was no indication of a 3 to 4 hour component.

As shown in Figure 9, no gamma photopeaks were clearly evident above background in the reaction products of Zr^{92} plus 14.7-Mev neutrons. Although some low-level gamma activity must certainly be present from the reaction products of other isotopes of zirconium in the separated sample of Zr^{92} and from any branching of the Y^{92} beta decay, it was masked by the background. This Zr^{92} sample, which was also counted under the end window Geiger counter, showed a 3.5-hour activity as expected from the beta decay of Y^{92}. A comparison of the two parts of Figure 9 indicates that a reaction involving Zr^{90} is the source of the 0.200- and 0.485-Mev gammas.

The level in Y^{90} at 0.200 Mev has also been reported by Bartholomew, Campion, Knowles, and Manning (Ref. 28). On the basis of angular correlation studies, these workers gave a tentative assignment of 3- to this level. As pointed out by Bocciolini, DiCaporiacco, Foa, and Mando (Ref. 25), the 3.1-hour activity is consistent with Weisskopf's lifetime formula if the 0.485-Mev gamma results from an M4 transition. These considerations would point to assignment of a 7 + level in Y^{90} at 0.685 Mev. The information on the decay of Y^{90m} is summarized in Figure 10 where possible shell model configurations are also indicated for the studied levels.

Niobium and Zirconium Cross Sections

The $Nb^{93}(n, 2n)Nb^{92}$, $Nb^{93}(n, \alpha)Y^{90m}$ and $Zr^{90}(n, p)Y^{90m}$ cross sections were found to be 360 ± 120 mb, 5 ± 2 mb, and 12 ± 4 mb respectively at 14.7 Mev. The absolute cross sections obtained for $Nb^{93}(n, 2n)Nb^{92}$ and $Nb^{93}(n, \alpha)Y^{90m}$ were based on a $Cu^{63}(n, 2n)Cu^{62}$ cross section of 586 mb at 14.7 Mev taken from Figure 11. The $Cu^{63}(n, 2n)Cu^{62}$ relative excitation function of Figure 11 was measured to supplement the present work and was normalized to the presently best available value of 534 mb at 14.3 Mev, which is a weighted average of several workers (Refs. 19, 20, 22, 24, 29 and 30). The $Zr^{90}(n, p)Y^{90m}$ cross section was based on a $Zr^{90}(n, 2n)Zr^{89}$ cross section of 822 mb (Ref. 31). In making the Nb and Zr cross section determinations, corrections were included for crystal efficiency, saturation factors,

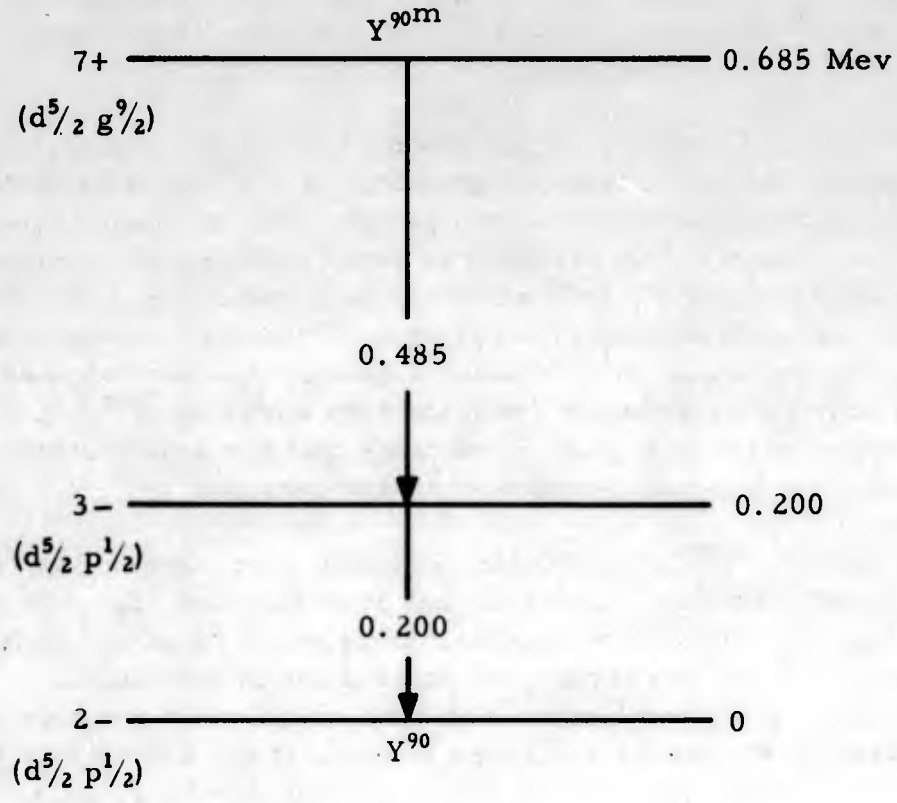

Figure 10. - Decay of Y^{90m}.

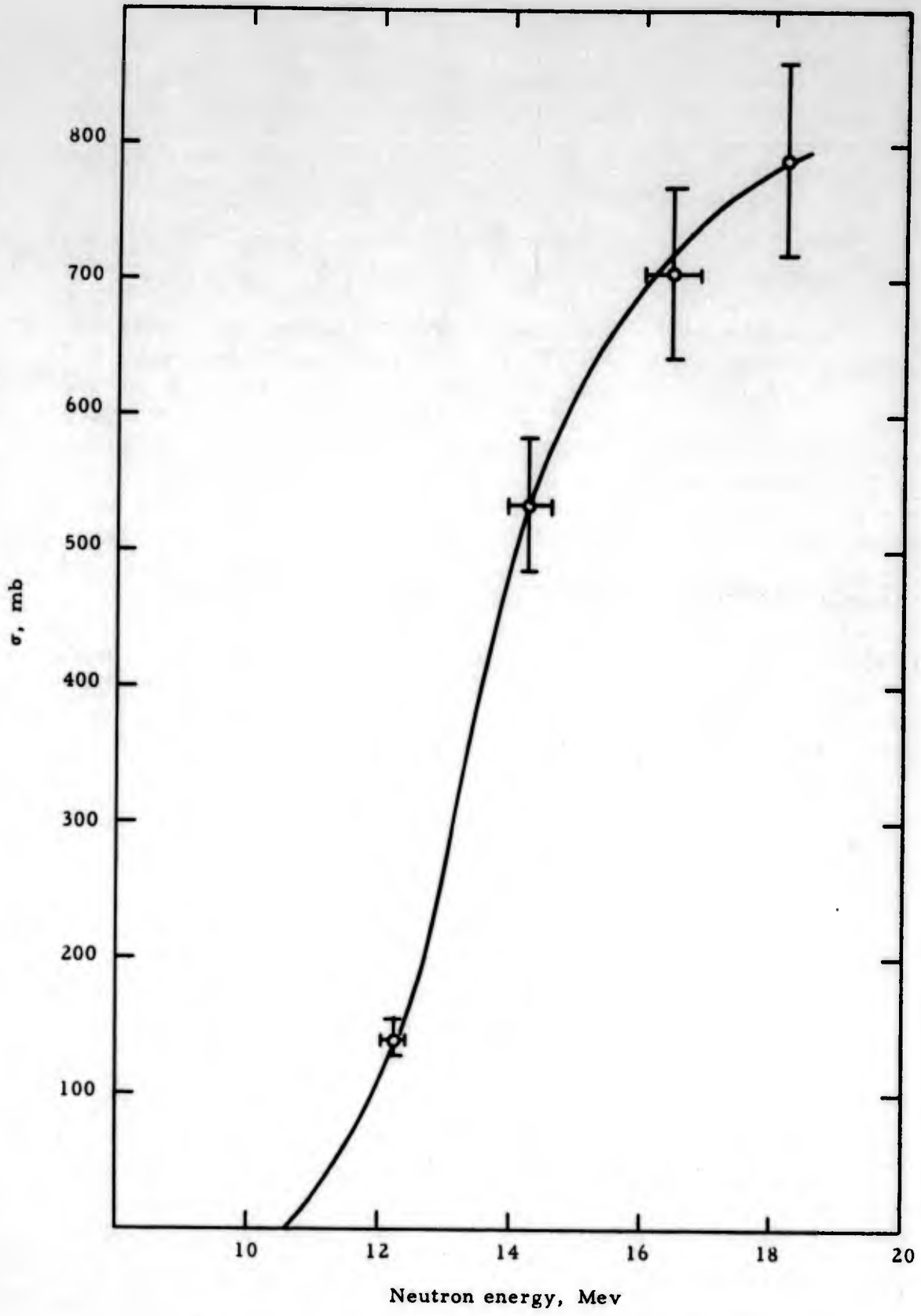

Figure 11. - Cu^{63} (n, 2n) Cu^{62} excitation function.

internal conversion coefficients (Ref. 32), and decay factors. It was found that, within the uncertainties in the crystal efficiencies and the internal conversion coefficients, the number of 0.485-Mev gamma rays was equal to the number of 0.200-Mev gamma rays. No measurements of these cross sections were made at the lower neutron energies; however, the yields were markedly reduced from those at 14.7-Mev neutron energy.

CONCLUSIONS

The experimental cross section results presented here are not in significant disagreement with the statistical model theoretical results, although in general, the experimental values are somewhat smaller than the theory predicts. Moreover, as pointed out in the introduction, a direct interaction process might be a possible mechanism in some instances. The manifestation of such a mechanism would be to reduce the (n, 2n) process since the ejected secondary particle would carry off the major portion of the incident energy leaving the intermediate nucleus energetically unable to emit a second particle. Furthermore, since such direct encounters result in a forward peaked distribution of the higher energy secondary particles, this description can be experimentally tested with techniques similar to those of Remy and Winter (Ref. 33). Such experiments are therefore proposed for further study of the nuclear reaction process in this energy region to help clarify the mechanisms involved.

The rather low experimental value obtained for the $Nb^{93}(n, 2n)$ cross section suggests further study of the energy levels in Nb^{92}. Either an extremely short or long lived isomeric state would account for the unexpected low value found for this cross section.

Appendix A

DERIVATION OF "APPROXIMATE" EXPRESSION FOR (n, 2n) CROSS SECTION,[15]

We make the assumption that competition from other reactions is small. Also, since we are considering the (n, 2n) process, the energy of excitation of the residual nucleus (after emission of first neutron) must be greater than the binding energy, E_b, of a neutron in the nucleus, i.e. $(E_n - \epsilon_n) > E_b$ in order that emission of a second neutron may be possible. When statistical considerations may be employed for both target and residual nuclei, then

$$\sigma(n, 2n) = \sigma_{in}(E_n) \frac{\int_0^{E_n - E_b} \epsilon_n \sigma_c(\epsilon_n) \omega(E_n - \epsilon_n) d\epsilon_n}{\int_0^{E_n} \epsilon_n \sigma_c(\epsilon_n) \omega(E_n - \epsilon_n) d\epsilon_n}$$

where $\sigma_{in}(E_n) \cong \sigma_c(E_n)$ if $E_n >> D_o$; D_o is the energy spacing of levels near the ground state in the residual nucleus.
Now,

$$\omega = C \exp 2\left(a[E_n - \epsilon_n]\right)^{1/2} = C \exp 2\left(aE_n\right)^{1/2}\left(1 - \frac{\epsilon_n}{E_n}\right)^{1/2}$$

We can approximate $\left(1 - \frac{\epsilon_n}{E_n}\right)^{1/2}$ by $1 - \frac{1}{2}\frac{\epsilon_n}{E_n}$, therefore,

$$\omega \cong C \exp\left[2\left(aE_n\right)^{1/2} - a^{1/2}\frac{\epsilon_n}{E_n^{1/2}}\right] = C \exp 2\left(aE_n\right)^{1/2} \exp\left(-\frac{a^{1/2}\epsilon_n}{E_n^{1/2}}\right)$$

The cross section $\sigma_c(\epsilon_n)$ is a slowly varying function of ϵ_n except near $\epsilon = 0$. We can therefore replace $\sigma_c(\epsilon_n)$ in the integrand by $\sigma_c(\epsilon_{max})$ where ϵ_{max} is the maximum of the function $\epsilon_n \omega(E_n - \epsilon_n)$. The denominator can then be evaluated as

$$\sigma_c\left(\sqrt{\frac{E_n}{a}}\right) C \exp 2(aE_n)^{1/2} \int_0^{E_n} \epsilon_n \exp\left(-\frac{a^{1/2}\epsilon_n}{E_n^{1/2}}\right) d\epsilon_n$$

$$= \sigma_c\left(\sqrt{\frac{E_n}{a}}\right) C \exp 2(aE_n)^{1/2} \left| \frac{\exp\left(-\frac{a^{1/2}}{E_n^{1/2}}\epsilon_n\right)}{a/E_n} \left(\frac{-\epsilon_n}{(E_n/a)^{1/2}} - 1\right) \right|_0^{E_n}$$

$$= \sigma_c\left(\sqrt{\frac{E_n}{a}}\right) C \exp 2(aE_n)^{1/2}\left[\frac{\exp(-)(aE_n)^{1/2}}{a/E_n}\left(-(aE_n)^{1/2} - 1\right) + \frac{E_n}{a}\right]$$

$$= \sigma_c\left(\sqrt{\frac{E_n}{a}}\right) C\left(\exp 2(aE_n)^{1/2}\right).(E_n/a) \text{ since } \exp\left(-(aE_n)^{1/2}\right) << 1$$

The numerator becomes

$$\int_0^{E_n - E_b} \sigma_c\left(\sqrt{\frac{E_n}{a}}\right)\epsilon_n\left(C \exp 2(aE_n)^{1/2}\right)\exp(-)\left(\frac{a^{1/2}\epsilon_n}{E_n^{1/2}}\right)d\epsilon_n$$

$$= \sigma_c\left(\sqrt{\frac{E_n}{a}}\right)\left(C \exp 2(aE_n)^{1/2}\right)\left|\frac{\exp(-)\left(\frac{a^{1/2}\epsilon_n}{E_n^{1/2}}\right)}{a/E_n}\left(-\frac{a^{1/2}}{E_n^{1/2}}\epsilon_n - 1\right)\right|_0^{E_n - E_b}$$

$$= \sigma_c\left(\sqrt{\frac{E_n}{a}}\right)\left(C \exp 2(aE_n)^{1/2}\right)\frac{E_n}{a}\left[1 - \left(1 + \frac{a^{1/2}}{E_n^{1/2}}[E_n - E_b]\right)\right.$$

$$\left.\exp(-)\left(\frac{a}{E_n}\right)^{1/2}(E_n - E_b)\right]$$

We then have

$$\sigma(n, 2n) = \sigma_{in}(E_n)\left[1 - \left(1 + \frac{\epsilon_c}{\theta}\right)\exp(-)(\epsilon_c/\theta)\right]$$

where

$$\epsilon_c = E_n - E_b \text{ and } \theta = \left(\frac{E_n}{a}\right)^{1/2}.$$

REFERENCES

1. Weisskopf, V. F.: AEC Rep. BNL-331, 1955 (unpublished).
2. Blatt, J. M. and Weisskopf, V. F.: Theoretical Nuclear Physics (John Wiley & Sons Inc., New York, 1952), p. 340.
3. Peaslee, D. C.: Annual Review of Nuclear Science (Annual Reviews Inc., Palo Alto, California, 1955), Vol. 5, p. 99.
4. Koehler, D. R. and Alford, W. L.: Bull. Am. Phys. Soc. 4, 405 (1959).
5. Koehler, D. R. and Alford, W. L.:Phys. Rev. 119, 311 (1960).
6. Alford, W. L. and Koehler, D. R.: Bull. Am. Phys. Soc. 5, 443 (1960).
7. Koehler, D. R.,Alford, W. L., and Mandeville, C. E.: Fast Neutron Induced Reactions in Nb and Zr, paper presented at Southeastern Section Meeting of American Physical Society in Louisville, March 30 - April 1, 1961.
8. Haskin, Larry, and Vandenbosch, Robert,: Phys. Rev. 123, 184 (1961).
9. Heath, R. L., Cline, J. E., Reich, C. W., Yates, E. C., and Turk, E. H.: Phys. Rev. 123, 903 (1961).
10. Lyons, W. S., Eldridge, J. S., and Bate, L. C.: Phys. Rev. 123, 1747 (1961).
11. Ferguson, J. M.: Nuclear Phys. 27, 344 (1961).
12. Carter-Waschek, C., and Linder, B.: Nuclear Phys. 27, 415 (1961).
13. Alford, W. L., Koehler, D. R.,and Mandeville, C. E.: Phys. Rev. 123, 1365 (1961).
14. Poularikas, A. and Fink, R. W.: Phys. Rev. 115, 989 (1959).
15. Feld, B. T., Feshbach, H., Goldberger, M. L., Goldstein, H., and Weisskopf, V. F.: Atomic Energy Commission Report NYO-636, 1951 (unpublished).
16. Bame, S. J. and Perry, J. E.: Phys. Rev. 107, 1616 (1957).
17. Cassatt, W. A., Jr., and Meinke, W. W.: Phys. Rev. 99, 760 (1955).
18. Rayburn, L. A.: Phys. Rev. 122, 168 (1961).

REFERENCES (Concluded)

19. Yasumi, S.: J. Phys. Soc. (Japan) 12, 443 (1957).

20. Paul, E. B. and Clarke, R. L.: Can. J. Phys. 31, 267 (1953).

21. Cohen, A. V. and White, P. H.: Nuclear Phys. 1, 73 (1956).

22. Forbes, S. G.: Phys. Rev. 88, 1309 (1952).

23. Ashby, V. J. and Catron, H. C.: Atomic Energy Commission Report UCRL-5419, 1959 (unpublished).

24. Ferguson, J. M. and Thompson, W. E.: Phys. Rev. 118, 228 (1960).

25. Bocciolini, M., Di Caporiacco, G., Foa, L., and Mando, M.: Nuovo Cimento 16, 780 (1960).

26. Strominger, D. Hollander, J. M. and Seaborg, G. T.: Revs. Modern Phys. 30, 636 (1958). Unless otherwise noted, decay scheme information was taken from this reference.

27. Howerton, R. J.: AEC Rep. UCRL-5351, 1958 (unpublished).

28. Bartholomew, G. A., Campion, P. J., Knowles, J. W. and Manning, G.: Nuclear Phys. 10, 590 (1959).

29. Fowler, J. L. and Slye, J. M., Jr.,: Phys. Rev. 77, 787 (1950).

30. Brolley,, E., Jr., Fowler, J. L., and Schlacks, L. K.: Phys. Rev. 88, 618 (1952).

31. Prestwood, R. J. and Bayhurst, B. P.: Phys. Rev. 121, 1438 (1961).

32. Rose, M. E.: Beta and Gamma-Ray Spectroscopy (K. Siegbahn, ed., North Holland Publishing Co., Amsterdam, 1955) p. 905.

33. Remy, E. and Winter, K.: Nuovo Cimento 9, 664 (1958).

DISTRIBUTION

	Copy
Director Air University Library Maxwell Air Force Base, Alabama	1
The Research Analysis Corporation 6935 Arlington Raod Bethesda 14, Maryland ATTN: Library	2
U. S. Atomic Energy Commission University of California Lawrence Radiation Laboratory Technical Information Division P. O. Box 808 Livermore, California	3
Commanding Officer U. S. Army Chemical Warfare Laboratories Army Chemical Center, Maryland ATTN: CWL Technical Library	4
Jet Propulsion Laboratory 4800 Oak Grove Drive Pasadena, California ATTN: Library	5
Central Intelligence Agency 2430 E Street, N. W. Washington 25, D. C. ATTN: OCR Mail Room	6, 7
Commanding General White Sands Missile Range, New Mexico ATTN: ORDBS-OM Technical Library	8-10
Commanding Officer Naval Ordnance Laboratory Corona, California ATTN: Documents Librarian	11

DISTRIBUTION (Continued)

	Copy
Commander, Air Force Cambridge Research Center AFSC L. G. Hanscom Field Bedford, Massachusetts ATTN: CROOTR	12
Commander, Rome Air Development Center Griffiss Air Force Base Rome, New York ATTN: RCRIE-5	13
Commanding General Aberdeen Proving Ground, Maryland ATTN: Library	14
Commanding General U. S. Army Signal Engineering Laboratories Fort Monmouth, New Jersey ATTN: Technical Document Center	15
National Aeronautics and Space Administration 1520 H Street, N. W. Washington 25, D. C. ATTN: Mr. B. A. Mulcahy, Division of Research Information	16-21
Director, U. S. Naval Research Laboratory Washington 25, D. C. ATTN: Code 2027	22, 23
Sandia Corporation, Livermore Laboratory P. O. Box 969 Livermore, California ATTN: Technical Library	24
U. S. Atomic Energy Commission Sandia Corporation P. O. Box 5800 Albuquerque, New Mexico	25

DISTRIBUTION (Continued)

	Copy
U. S. Atomic Energy Commission Los Alamos Scientific Laboratory P. O. Box 1663 Los Alamos, New Mexico ATTN: Miss Helen Redman	26
Commander, Air Technical Intelligence Center Wright-Patterson Air Force Base, Ohio ATTN: AFOIN-4Bla	27
Commanding Officer, Picatinny Arsenal Dover, New Jersey ATTN: Technical Information Library	28
Commander, Armed Services Technical Information Agency Arlington Hall Station Arlington 12, Virginia ATTN: TIPCR	29-38
Director National Security Agency Fort George G. Meade, Maryland ATTN: CREF, Technical Documents Section	39
Commanding General U. S. Army Engineer Research and Development Laboratories Fort Belvoir, Virginia ATTN: Technical Documents Center	40
U. S. Atomic Energy Commission Technical Reports Library Washington 25, D. C. ATTN: J. M. O'Leary	41

DISTRIBUTION (Continued)

	Copy
Commanding General, Field Command Defense Atomic Support Agency Sandia Base P. O. Box 5100 Albuquerque, New Mexico ATTN: Development Division	42
Air Force Office of Scientific Research Temporary T Building 14th Street and Constitution Avenue, N. W. Washington 25, D. C. ATTN: SREC	43
Manager, Albuquerque Operations U. S. Atomic Energy Commission P. O. Box 5400 Albuquerque, New Mexico	44
U. S. Atomic Energy Commission Technical Information Service Extension P. O. Box 62 Oak Ridge, Tennessee	45
Chief, Defense Atomic Support Agency Washington 25, D. C. ATTN: Documents Library Branch	46
Commanding Officer Watertown Arsenal Wate. town 72, Massachusetts ATTN: Ordnance Materials Research Office	47
Dr. J. L. Martin	48
Mr. J. A. Hofmann	49
Mr. Homer Priest	50
Laboratory	51
Mr. N. L. Reed	52
Mr. G. A. Darcy	53
Mr. P. Sagalyn	54

DISTRIBUTION (Continued)

	Copy
Commanding Officer U. S. Army Research Office (Durham) Box CM Duke Station Durham, North Carolina	
ATTN: Dr. J. W. Dawson	55
Dr. S. Githens	56-58
Mr. G. Cox	59
Commanding Officer Watervliet Arsenal Watervliet, New York	
ATTN: Mr. P. M. Netzer	60
Dr. Fritz Sautter	61
Commanding Officer Ordnance Tank-Auto Command 1501 Beard Street Detroit 9, Michigan	
ATTN: Mr. S. H. Fuller	62
Mr. Fred Seppi	63
Mr. P. Hoffman-Pinther	64
Commanding General USA Ordnance Arsenal Frankford Philadelphia 37, Pennsylvania	
ATTN: Mr. W. J. Kroeger	65
Mr. M. Weinstock - 1421-5583	66
Dr. M. L. Chwalow	67
Commanding Officer Diamond Ordnance Fuze Laboratories Washington 25, D. C.	
ATTN: Mr. M. Apstein	68
Technical Reference Section	69
Commanding General Ordnance Weapons Command Rock Island, Illinois	
ATTN: Mr. W. G. Smith	70

DISTRIBUTION (Continued)

	Copy
Commanding Officer Picatinny Arsenal Dover, New Jersey ATTN: Mr. S. Verner	71
Mr. W. R. Carson	72
Mr. S. Penn	73
Director Waterways Experiment Station Vicksburg, Mississippi ATTN: Research Center Library	74
Quartermaster Research and Engineering Laboratories Natick, Massachusetts ATTN: Dr. J. M. Davies	75
The Johns Hopkins University Operations Research Office 6935 Arlington Road Bethesda, Maryland ATTN: Dr. T. S. Needels	76
Dr. B. B. Watson	77
Dr. Arthur E. Ruark Chief, Controlled Thermonuclear Branch Division of Research U. S. Atomic Energy Commission Washington 25, D. C.	78
Exchange and Gift Division Library of Congress Washington 25, D. C.	79
CONVAIR Scientific Research Laboratory A Division of General Dynamics Corporation 5001 Kearney Villa Road San Diego 11, California ATTN: Mr. A. L. Berlad	80

DISTRIBUTION (Continued)

	Copy
Geophysics Corporation of America 700 Commonwealth Avenue Boston 15, Massachusetts ATTN: Mr. R. M. Chapman, Director of Engineering	81
AVCO Research Laboratory 2385 Revere Beach Parkway Everett 49, Massachusetts ATTN: Librarian	82
Saint Louis University 221 N. Grand, St. Louis, Missouri ATTN: Mr. A. H. Weber, Physics Dept.	83
James Forrestal Research Center Princeton University, P. O. Box 451 Princeton, New Jersey	84
University of Alabama University, Alabama ATTN: Dr. F. H. Mitchell, Box 1392	85
Dr. J. Richard Haskins Gettysburg College Gettysburg, Pennsylvania	86
Armour Research Foundation Illinois Institute of Technology Technical Center 10 W. 35th Street Chicago 16, Illinois	87
George C. Marshall Space Flight Center National Aeronautics and Space Administration Redstone Arsenal, Alabama ATTN: M-RP-DIR	88
M-RP-N	89

DISTRIBUTION (Concluded)

		Copy
Commanding General		
U. S. Army Ordnance Missile Command		
Redstone Arsenal, Alabama		
ATTN:	ORDXM-XS	90
	ORDXM-R	91
	ORDXM-RM	92
	ORDXM-RF	93
	ORDXM-RR	94-118
	ORDXM-RB	119-121
	ORDXM-RAP	122

AD_____ Accession No. _____

Army Ordnance Missile Command, Research & Development Directorate, Research Laboratory, Redstone Arsenal, Alabama

NEUTRONS PARTIAL CROSS SECTION STUDIES - D. R. Koehler and W. L. Alford

AOMC RR-TR-62-1, 10 Apr 62, 34 pp - illus. Unclassified Report

The (n, 2n) excitation functions are given for Zn^{64}, Br^{79}, Ag^{107}, Sb^{121}, and Pr^{141}. Evidence is presented for a 7+ isomeric state in Y^{90} at 0.685 Mev. $Zr^{90}(n, p)Y^{90m}$ and $Nb^{93}(n, \alpha)Y^{90m}$ cross sections for 14.7 -Mev neutrons are reported to be 12 ± 4 mb and 5 ± 2 mb, respectively.

Unclassified
1. Neutron cross sections
2. Nuclear reactions--Analysis
I. Koehler, D. R.
II. Alford, W. L.

DISTRIBUTION: Copies obtainable from ASTIA Arlington Hall Station, Arlington 12, Virginia

AD_____ Accession No. _____

Army Ordnance Missile Command, Research & Development Directorate, Research Laboratory, Redstone Arsenal, Alabama

NEUTRONS PARTIAL CROSS SECTION STUDIES - D. R. Koehler and W. L. Alford

AOMC RR-TR-62-1, 10 Apr 62, 34 pp - illus. Unclassified Report

The (n, 2n) excitation functions are given for Zn^{64}, Br^{79}, Ag^{107}, Sb^{121}, and Pr^{141}. Evidence is presented for a 7+ isomeric state in Y^{90} at 0.685 Mev. $Zr^{90}(n, p)Y^{90m}$ and $Nb^{93}(n, \alpha)Y^{90m}$ cross sections for 14.7 -Mev neutrons are reported to be 12 ± 4 mb and 5 ± 2 mb, respectively.

Unclassified
1. Neutron cross sections
2. Nuclear reactions--Analysis
I. Koehler, D. R.
II. Alford, W. L.

DISTRIBUTION: Copies obtainable from ASTIA Arlington Hall Station, Arlington 12, Virginia

AD_____ Accession No. _____

Army Ordnance Missile Command, Research & Development Directorate, Research Laboratory, Redstone Arsenal, Alabama

NEUTRONS PARTIAL CROSS SECTION STUDIES - D. R. Koehler and W. L. Alford

AOMC RR-TR-62-1, 10 Apr 62, 34 pp - illus. Unclassified Report

The (n, 2n) excitation functions are given for Zn^{64}, Br^{79}, Ag^{107}, Sb^{121}, and Pr^{141}. Evidence is presented for a 7+ isomeric state in Y^{90} at 0.685 Mev. $Zr^{90}(n, p)Y^{90m}$ and $Nb^{93}(n, \alpha)Y^{90m}$ cross sections for 14.7 -Mev neutrons are reported to be 12 ± 4 mb and 5 ± 2 mb, respectively.

Unclassified
1. Neutron cross sections
2. Nuclear reactions--Analysis
I. Koehler, D. R.
II. Alford, W. L.

DISTRIBUTION: Copies obtainable from ASTIA Arlington Hall Station, Arlington 12, Virginia

AD_____ Accession No. _____

Army Ordnance Missile Command, Research & Development Directorate, Research Laboratory, Redstone Arsenal, Alabama

NEUTRONS PARTIAL CROSS SECTION STUDIES - D. R. Koehler and W. L. Alford

AOMC RR-TR-62-1, 10 Apr 62, 34 pp - illus. Unclassified Report

The (n, 2n) excitation functions are given for Zn^{64}, Br^{79}, Ag^{107}, Sb^{121}, and Pr^{141}. Evidence is presented for a 7+ isomeric state in Y^{90} at 0.685 Mev. $Zr^{90}(n, p)Y^{90m}$ and $Nb^{93}(n, \alpha)Y^{90m}$ cross sections for 14.7 -Mev neutrons are reported to be 12 ± 4 mb and 5 ± 2 mb, respectively.

Unclassified
1. Neutron cross sections
2. Nuclear reactions--Analysis
I. Koehler, D. R.
II. Alford, W. L.

DISTRIBUTION: Copies obtainable from ASTIA, Arlington Hall Station, Arlington 12, Virginia

AD ____________ Accession No. ____________

Army Ordnance Missile Command, Research & Development Directorate, Research Laboratory, Redstone Arsenal, Alabama

NEUTRONS PARTIAL CROSS SECTION STUDIES - D. R. Koehler and W. L. Alford

AOMC RR-TR-62-1, 10 Apr 62, 34 pp - illus.
Unclassified Report

The (n, 2n) excitation functions are given for Zn^{64}, Br^{79}, Ag^{107}, Sb^{121}, and Pr^{141}. Evidence is presented for a 7+ isomeric state in Y^{90} at 0.685 Mev. $Zr^{90}(n, p)Y^{90m}$ and $Nb^{93}(n, \alpha)Y^{90m}$ cross sections for 14.7 -Mev neutrons are reported to be 12 ± 4 mb and 5 ± 2 mb, respectively.

Unclassified

1. Neutron cross sections
2. Nuclear reactions--Analysis

I. Koehler, D. R.
II. Alford, W. L.

DISTRIBUTION: Copies obtainable from ASTIA Arlington Hall Station, Arlington 12, Virginia

AD ____________ Accession No. ____________

Army Ordnance Missile Command, Research & Development Directorate, Research Laboratory, Redstone Arsenal, Alabama

NEUTRONS PARTIAL CROSS SECTION STUDIES - D. R. Koehler and W. L. Alford

AOMC RR-TR-62-1, 10 Apr 62, 34 pp - illus.
Unclassified Report

The (n, 2n) excitation functions are given for Zn^{64}, Br^{79}, Ag^{107}, Sb^{121}, and Pr^{141}. Evidence is presented for a 7+ isomeric state in Y^{90} at 0.685 Mev. $Zr^{90}(n, p)Y^{90m}$ and $Nb^{93}(n, \alpha)Y^{90m}$ cross sections for 14.7 -Mev neutrons are reported to be 12 ± 4 mb and 5 ± 2 mb, respectively.

Unclassified

1. Neutron cross sections
2. Nuclear reactions--Analysis

I. Koehler, D. R.
II. Alford, W. L.

DISTRIBUTION: Copies obtainable from ASTIA, Arlington Hall Station, Arlington 12, Virginia

AD ____________ Accession No. ____________

Army Ordnance Missile Command, Research & Development Directorate, Research Laboratory, Redstone Arsenal, Alabama

NEUTRONS PARTIAL CROSS SECTION STUDIES - D. R. Koehler and W. L. Alford

AOMC RR-TR-62-1, 10 Apr 62, 34 pp - illus.
Unclassified Report

The (n, 2n) excitation functions are given for Zn^{64}, Br^{79}, Ag^{107}, Sb^{121}, and Pr^{141}. Evidence is presented for a $7 \pm$ isomeric state in Y^{90} at 0.685 Mev. $Zr^{90}(n, p)Y^{90m}$ and $Nb^{93}(n, \alpha)Y^{90m}$ cross sections for 14.7 -Mev neutrons are reported to be 12 ± 4 mb and 5 ± 2 mb, respectively.

Unclassified

1. Neutron cross sections
2. Nuclear reactions--Analysis

I. Koehler, D. R.
II. Alford, W. L.

DISTRIBUTION: Copies obtainable from ASTIA Arlington Hall Station, Arlington 12, Virginia

AD ____________ Accession No. ____________

Army Ordnance Missile Command, Research & Development Directorate, Research Laboratory, Redstone Arsenal, Alabama

NEUTRONS PARTIAL CROSS SECTION STUDIES - D. R. Koehler and W. L. Alford

AOMC RR-TR-62-1, 10 Apr 62, 34 pp - illus.
Unclassified Report

The (n, 2n) excitation functions are given for Zn^{64}, Br^{79}, Ag^{107}, Sb^{121}, and Pr^{141}. Evidence is presented for a 7+ isomeric state in Y^{90} at 0.685 Mev. $Zr^{90}(n, p)Y^{90m}$ and $Nb^{93}(n, \alpha)Y^{90m}$ cross sections for 14.7 -Mev neutrons are reported to be 12 ± 4 mb and 5 ± 2 mb, respectively.

Unclassified

1. Neutron cross sections
2. Nuclear reactions--Analysis

I. Koehler, D. R.
II. Alford, W. L.

DISTRIBUTION: Copies obtainable from ASTIA, Arlington Hall Station, Arlington 12, Virginia

UNCLASSIFIED